



OPEN

CONFERENCE
PROCEEDINGS

ACSMS2014

.....

SUBJECT AREAS:

MATERIALS SCIENCE

ENVIRONMENTAL SCIENCES

Received

1 September 2014

Accepted

13 November 2014

Published

4 December 2014

Correspondence and requests for materials should be addressed to DY. (d.yang@qdu.edu.cn) or XY. (x.yao@griffith.edu.au)

Potassium Niobate Nanolamina: A Promising Adsorbent for Entrapment of Radioactive Cations from Water

Jin Sun¹, Dongjiang Yang^{1,3}, Cuihua Sun¹, Long Liu¹, Shuanglei Yang², Yi (Alec) Jia³, Rongsheng Cai⁴ & Xiangdong Yao³

¹Collaborative Innovation Centre for Marine Biomass Fibres, Materials and Textiles of Shandong Province; College of Chemical and Environmental Engineering, Qingdao University, Qingdao, P R China, ²State Key Laboratory for Powder Metallurgy, Central South University, Changsha 410083, People's Republic of China, ³Queensland Micro- and Nanotechnology Centre (QMNC), Griffith University, Nathan, Brisbane, Queensland 4111, Australia, ⁴Nanoscale Physics Research Laboratory, School of Physics and Astronomy, University of Birmingham, Birmingham, B15 2TT, United Kingdom.

Processing and managing radioactive waste is a great challenge worldwide as it is extremely difficult and costly; the radioactive species, cations or anions, leaked into the environment are a serious threat to the health of present and future generations. We report layered potassium niobate ($K_4Nb_6O_{17}$) nanolamina as adsorbent to remove toxic Sr^{2+} , Ba^{2+} and Cs^+ cations from wastewater. The results show that $K_4Nb_6O_{17}$ nanolamina can permanently confine the toxic cations within the interlayer spacing via a considerable deformation of the metastable layered structure during the ion exchange process. At the same time, the nanolaminar adsorbent exhibits prompt adsorption kinetics, high adsorption capacity and selectivity, and superior acid resistance. These merits make it be a promising material as ion exchanger for the removal of radioactive cations from wastewater.

With increasing applications of nuclear technology, radioactive contaminants, especially in water, have become a huge threat to human health and the environment. For example, $^{226}Ra^{2+}$ ions from the tailings and heap-leach residues of uranium mining industry, $^{90}Sr^{2+}$ from the byproduct of nuclear fission reaction, and $^{137}Cs^+$ from the leakage of the nuclear reactor discharged to water can cause serious problems and need proper treatment¹⁻⁶. Given that the radioactivity of the radionuclides only declines with time, the traditional way to decontaminate radioactive liquid waste is removing the radionuclides for further disposal. Among all these techniques, ion exchange is of high efficiency and convenience. Thus it has become the most promising method. There is an ongoing effort to develop efficient materials as ion exchangers for the treatment of radioactive liquid waste. Natural inorganic cation exchangers, such as clays and zeolites^{7,8}, and synthetic inorganic materials, such as synthetic γ -zirconium phosphate¹, micas^{2,4}, niobate molecular sieves^{5,6} and titanate nanomaterials⁹⁻¹⁶, have been extensively studied for this purpose. It is important for the ion exchangers to possess high exchange capacity, possible selectivity and specificity, and good resistant to radiation. More importantly, a metastable structure like layered or tunnel, which may collapse after ion exchange and then assures the toxic ions are permanently trapped, is definitely desirable¹¹⁻¹⁶. This assures that the adsorbed radioactive species could not be released from the adsorbents, and thus avoids secondary pollution.

In the present work, $K_4Nb_6O_{17}$ nanolamina was synthesized by a wet chemical reaction between niobium oxide and alkali hydroxides under hydrothermal conditions. $K_4Nb_6O_{17}$ has a typical layered perovskite-like structure that is composed of twisted NbO_6 octahedral units¹⁷⁻¹⁹. As shown in Scheme S1, the NbO_6 octahedral form layers that carry negative electrical charges by sharing edges or corners. These layers stack along b axis direction and exchangeable K^+ cations are filled in the interlayers to compensate for the negative charges of the NbO_6 sheets. The unit cell of $K_4Nb_6O_{17}$ contains four layers and two types of interlayer regions, denoted by interlayer I and interlayer II^{20,21}. The cation exchange capacity (CEC) for bivalent and univalent cations of $K_4Nb_6O_{17}$ is 2.03 and 4.06 mmol/g, respectively. This CEC value is relatively higher than the ones belonging to the conventional inorganic ion exchangers such as layered clays, zeolites, and γ -ZrP, which have CEC values in a range between 0.4 and 1.6 mmol/g¹⁻⁴. The $K_4Nb_6O_{17}$ nanolamina was used as adsorbent to trap Sr^{2+} , Ra^{2+} and Cs^+ from aqueous solution. It was found that the $K_4Nb_6O_{17}$ nanolamina exhibited high adsorption capacity, selectivity, and fast kinetics, which indicates that it is a high potential candidate as highly efficient adsorbent for radioactive cations.



Given the high toxicity of radioactive isotopes, we used aqueous solutions of non-radioactive ions, i.e., Cs^+ and Sr^{2+} in our sorption experiments instead. Non-radioactive Ba^{2+} cations can be used to simulate the adsorption behavior of Ra^{2+} ions due to a similar ionic diameter to radioactive Ra^{2+} ions and similar ion exchange behavior²². As presented in Figure 1a, the adsorption isotherms approach a plateau that is the experimental saturated adsorption capacity. For the adsorption of divalent Sr^{2+} and Ba^{2+} ions, the saturated capacities are ~ 1.78 and ~ 1.50 mmol/g, respectively. Apparently, the saturation capacities of Sr^{2+} and Ba^{2+} cations are slightly lower than the theoretical CEC values, that is, about 87% of the calculated value for Sr^{2+} sorption and 74% for Ba^{2+} cations. However, the saturated adsorption capacity for Cs^+ ions is ~ 1.25 mmol/g, which means only 31% of the K^+ ions are exchanged by the toxic Cs^+ ions and a large fraction of the K^+ ions are still retained between the $\text{K}_4\text{Nb}_6\text{O}_{17}$ nanolamina interlayers as the sorption reached saturation. This result is similar to the adsorption by layered or tunneled sodium titanate nanofibers and nanotube^{11–16}, where only 1/3 of the Na^+ ions can be exchanged by monovalent Cs^+ ions.

The morphology of the $\text{K}_4\text{Nb}_6\text{O}_{17}$ nanolamina before and after sorption of Cs^+ , Sr^{2+} and Ba^{2+} ions was observed by field emission scanning electron microscopy (FESEM). The composition of the samples was determined by energy-dispersive X-ray spectroscopy (EDS) attached on the same microscopy. As shown in Figure 2, the $\text{K}_4\text{Nb}_6\text{O}_{17}$ nanolamina is composed of two-dimensional niobate sheets with a parallel layered structure. After ion exchange with Cs^+ , Sr^{2+} and Ba^{2+} ions, the $\text{K}_4\text{Nb}_6\text{O}_{17}$ nanolamina maintains the laminar morphology. The laminar morphology possesses very important advantages for application in removal of toxic ions from water. For instance, laminar adsorbents can readily be dispersed into a solution and are easily accessed by the toxic cations. This property is able to enhance the kinetic of the sorption process. As shown in Fig. 1b, using adsorption time as the horizontal axis, we plotted the kinetic curves of Cs^+ , Sr^{2+} and Ba^{2+} ions adsorption. Obviously, all three toxic cations can reach sorption equilibrium within the first 5 hours and over 50% of equilibrium amount of adsorbed Sr^{2+} and Ba^{2+} ions were taken up within 1 hour. Compared with traditional ion exchangers, for example, $\gamma\text{-ZrP}$ and synthetic clays^{1–4}, the $\text{K}_4\text{Nb}_6\text{O}_{17}$ nanolamina is more efficient, in terms of adsorption kinetics, for the removal of radioactive cations from contaminated water. Additionally, the adsorbed Cs^+ , Sr^{2+} and Ba^{2+} ions have been verified by the EDS spectra (insets in Figure 2). The signal of

remained K^+ ions in Cs^+ exchanged sample is much higher than those of the Sr^{2+} and Ba^{2+} exchanged nanolaminas. This is in good agreement with the adsorption data shown in Figure 1a.

To explain the incomplete ion exchange, we compared the XRD patterns of the $\text{K}_4\text{Nb}_6\text{O}_{17}$ nanolamina before and after ion exchange (see Figure 3a). The main difference among the XRD patterns of the $\text{K}_4\text{Nb}_6\text{O}_{17}$ nanolamina before and after adsorption of Cs^+ , Sr^{2+} and Ba^{2+} ions is the shift of the first diffraction peak positioned at 8.56° which is assigned to (040) plane of $\text{K}_4\text{Nb}_6\text{O}_{17}$. As shown in Figure 3b, the d_{040} spacing is the interlayer spacing of $\text{K}_4\text{Nb}_6\text{O}_{17}$ nanolamina. For instance, the pristine $\text{K}_4\text{Nb}_6\text{O}_{17}$ nanolamina possesses a d_{040} spacing of 1.034 nm and it decreases to 0.956 nm when 87% of exchange sites in the nanolamina are occupied by Sr^{2+} ions, and decreases to 0.964 nm when the Ba^{2+} ion absorption is equivalent to 74% of the theoretical capacity. However, the d_{040} spacing only slightly decreases to 1.006 nm after reached Cs^+ adsorption equilibrium, since only 31% of exchange K^+ ions in the nanolamina are occupied by Cs^+ ions. The considerable deformation of the interlayer spacing indicates substantial structural changes of the nanolamina, which prevent further uptake of the toxic cations and is responsible for the incomplete exchange. This result is similar to the situation of titanate nano-adsorbents^{11–16} and synthetic micas²⁴. The collapse of the interlayer spacing by about 0.078, 0.070, and 0.028 nm for Sr^{2+} , Ba^{2+} , and Cs^+ , respectively, can be explained dehydration of the adsorbed cations owing to the extremely high charge density of the layers coupled with the relatively low hydration energy of the radioactive cations^{23–26}. Just as the toxic cations cannot enter the structure after initial ion exchange, the toxic cations that entered the $\text{K}_4\text{Nb}_6\text{O}_{17}$ nanolamina cannot escape from the collapsed interlayers, that is, effectively resulting in the confinement of the toxic Cs^+ , Sr^{2+} , and Ba^{2+} ions.

The structures of $\text{K}_4\text{Nb}_6\text{O}_{17}$ nanolamina after sorption of Cs^+ , Sr^{2+} , and Ba^{2+} ions were also analyzed by high resolution transmission electron microscopy (HRTEM), and the analysis provides evidence of the structural deformation caused by cations sorption. Figure 4a shows nanolamina TEM image of the pristine $\text{K}_4\text{Nb}_6\text{O}_{17}$ with average size of several hundreds of nanometers. Figure 4b–d confirm that the laminar morphology is maintained after the adsorption of Cs^+ , Sr^{2+} , and Ba^{2+} ions. The HRTEM images (see Figure 4e–h) and the fast fourier transform (FFT) images (insets) also reveal more subtle structural changes induced by the entrapment of toxic cations. Apparently, one set of the fringe spacing of 0.323 nm is

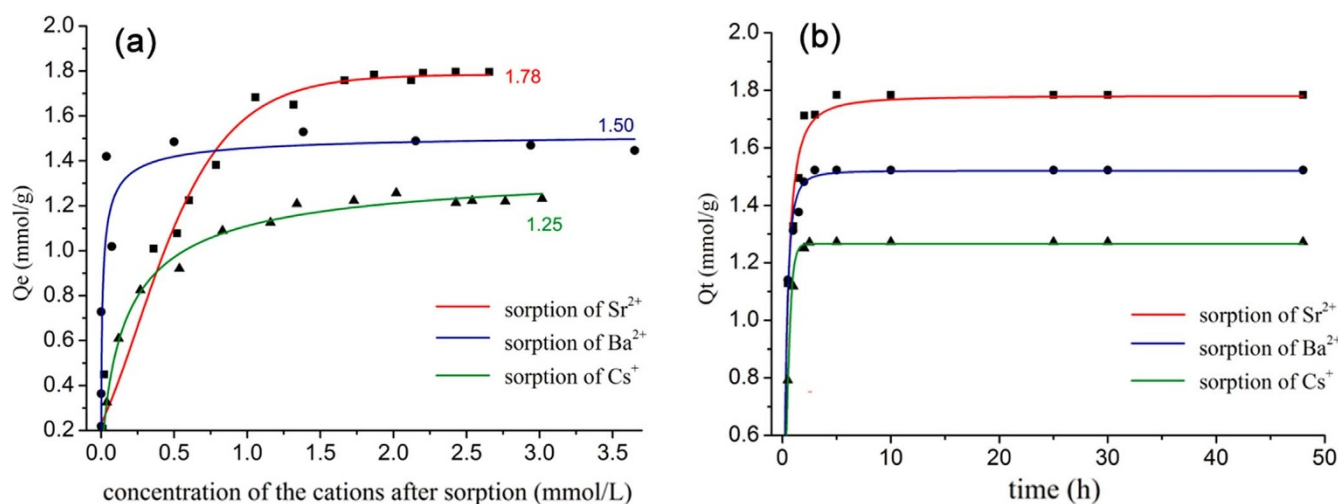


Figure 1 | (a) The isotherms of Sr^{2+} , Ba^{2+} , and Cs^+ absorption by $\text{K}_4\text{Nb}_6\text{O}_{17}$ nanolamina. The horizontal axis represents the concentration of the cations (mmol/L) remained in solution, while the vertical axis shows the saturation capacity (mmol/g) after reaching the sorption equilibrium. (b) The dynamic curves of Sr^{2+} , Ba^{2+} and Cs^+ sorption by $\text{K}_4\text{Nb}_6\text{O}_{17}$ nanolamina. The horizontal axis represents the sorption time, while the vertical axis shows the amount of the cations taken up by the adsorbent.

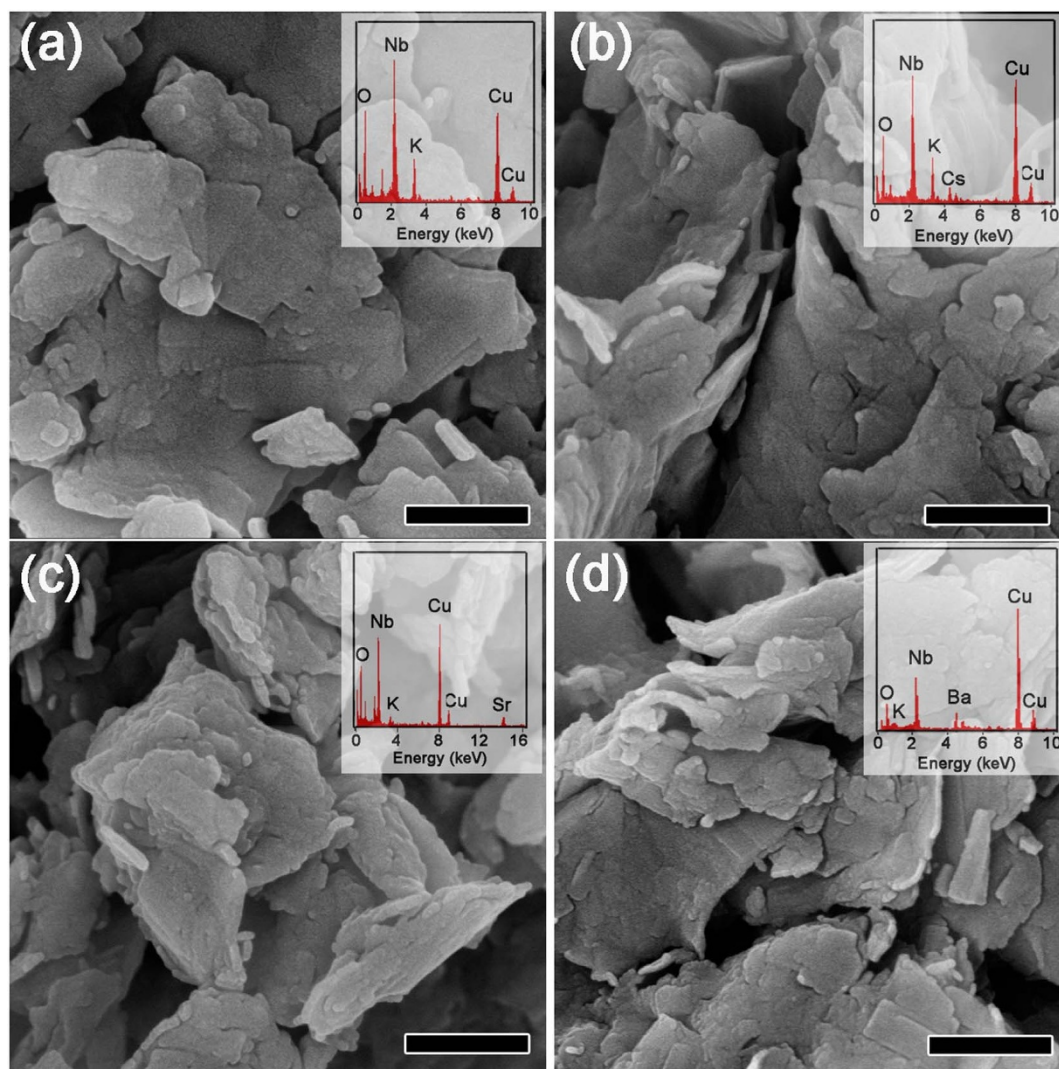


Figure 2 | FESEM images and EDS spectra (insets) of (a) the pristine $K_4Nb_6O_{17}$ nanolamina and the sample after adsorption of (b) Cs^+ , (c) Sr^{2+} and (d) Ba^{2+} ions. The scale bar on this drawing represents a length of 400 nm.

observed from the HRTEM image of the pristine $K_4Nb_6O_{17}$ (see Figure 4e), which is corresponding to the (002) plane of $K_4Nb_6O_{17}$. There is little defect and distortion in the crystal lattice. However,

after adsorption of Cs^+ , Sr^{2+} , and Ba^{2+} ions, obvious lattice distortion is observed. Additionally, the fringe spacing of (002) expands to 0.330 nm for the $K_4Nb_6O_{17}$ nanolamina after adsorption of Ba^{2+}

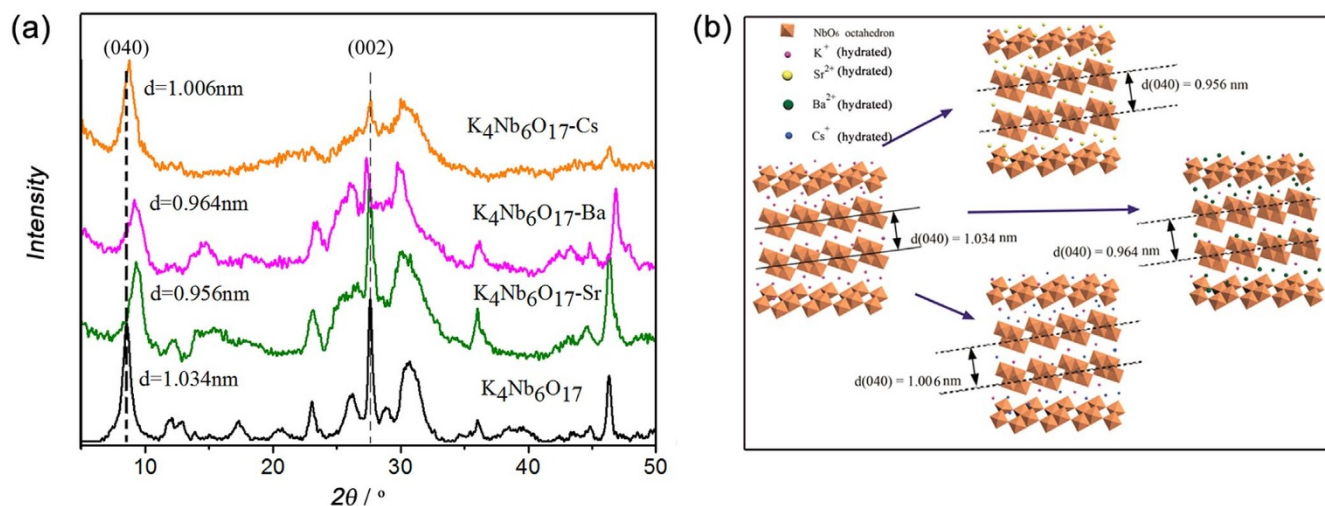


Figure 3 | (a) The XRD patterns of the $K_4Nb_6O_{17}$ nanolaminas before and after ion exchange. (b) Schematic illustration of the ion exchange between K^+ ions and the target cations.

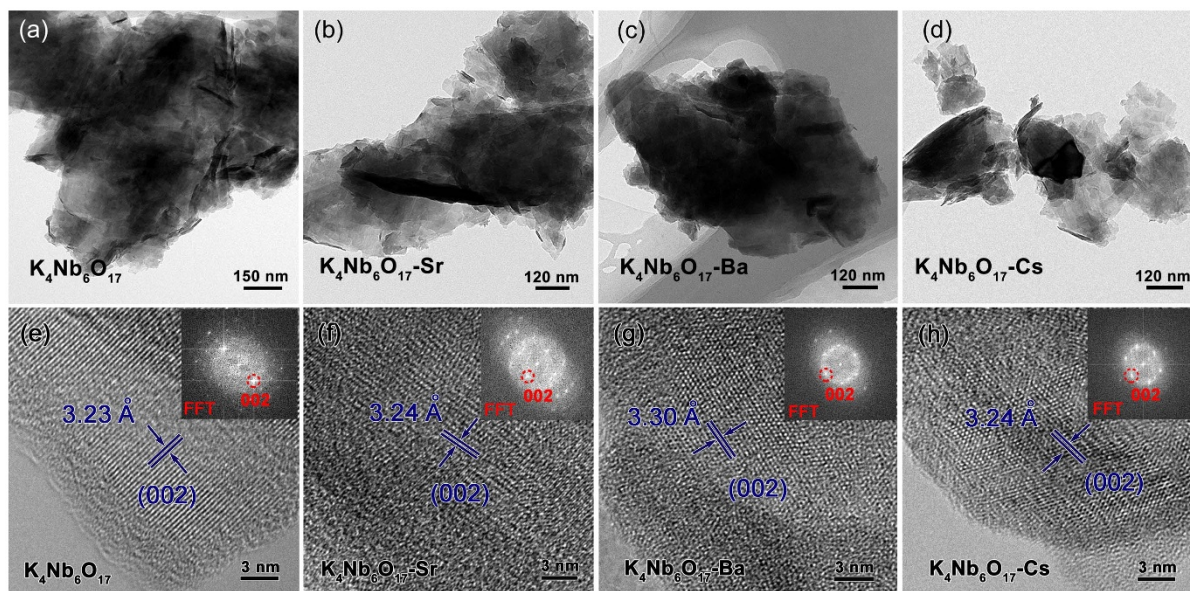


Figure 4 | TEM and HRTEM images of the $K_4Nb_6O_{17}$ nanolaminas: (a,e) the pristine $K_4Nb_6O_{17}$ and the sample after adsorption of (b,f) Sr^{2+} , (c,g) Ba^{2+} , and (d,h) Cs^+ ions. Insets: FFT images of the samples.

ions. This result is in good agreement with those of the XRD patterns where the diffraction peak of (002) plane shifts to lower angle after adsorption of Ba^{2+} ions (see Figure 3a).

The structural changes also lead to the desirable outcome that the toxic cations are trapped in the interlayer space permanently and safely for subsequently disposal. To verify the permanent trapping of the toxic cations in $K_4Nb_6O_{17}$ nanolamina, the adsorbent with equilibrium amount of Cs^+ , Sr^{2+} and Ba^{2+} ions were separated by centrifugation, washed with a small amount of water and then dispersed in water again. After stirring the suspension for 48 h, we measured the toxic ions concentration of the solution by atomic adsorption spectroscopy (AAS). As expected, only a small amount of target cations were released to the solution, that is, 3.2% of Sr^{2+} , 4.5% of Ba^{2+} and 1.3% Cs^+ , respectively. To determine the amount of the absorbed toxic ions remained in the $K_4Nb_6O_{17}$ nanolamina, the $K_4Nb_6O_{17}$ nanolamina with absorbed toxic cations after the release experiment were dissolved into 15 M HNO_3 solution and the concentrations of Cs^+ , Sr^{2+} and Ba^{2+} ions in the HNO_3 solution were measured by AAS. It was found that more than 90% of the absorbed toxic cations remained in the $K_4Nb_6O_{17}$ nanolamina. It is indicated that the structural deformation of the $K_4Nb_6O_{17}$ nanolamina resulted from the adsorption of these ions is beneficial for the permanent entrapment of target cations.

The adsorption selectivity of $K_4Nb_6O_{17}$ nanolamina to adsorb Cs^+ , Sr^{2+} , and Ba^{2+} ions in the presence of a large excess of K^+ ions was also investigated by equilibrating the adsorbent for 2 days within a solution containing 200 ppm Sr^{2+} (or 500 ppm Ba^{2+} , 150 ppm Cs^+) and K^+ ions (KNO_3 or KCl) of a concentration of 0 M, 0.01 M, 0.05 M and 0.1 M at room temperature. The distribution coefficient K_d^{27} , which is the ratio of the metal ions adsorbed into the adsorbent (per gram) to the metal remaining in solution (per milliliter), is listed in Table 1. The existence of a small amount of K^+ ions can cause significant decrease of all three toxic cations adsorption. However, further increase of K^+ ions concentration only results in a relatively slight decrease of the metal ions sorption and the K_d values, particularly for the divalent cations. This means the $K_4Nb_6O_{17}$ nanolamina possesses good adsorption selectivity. Similar results were obtained in the presence of a large amount of competitive Na^+ and Ca^{2+} ions. As shown in Table S1 and S2, the K_d values of $K_4Nb_6O_{17}$ nanolamina are highly influenced by the divalent Ca^{2+} ions in comparison with monovalent K^+ and Na^+ ions.

In addition, given radioactive liquid waste is usually an acidic solution, for example, $^{137}Cs^+$ and $^{90}Sr^{2+}$ acidic aqueous solution²⁸, it is very important for the adsorbents used to decontaminate the liquid waste to possess acid resistance and stay ion exchangeable in acidic environment. To investigate the influence of the pH value on the sorption of Cs^+ , Sr^{2+} , and Ba^{2+} ions, we equilibrated $K_4Nb_6O_{17}$ nanolamina for 2 days within a solution under a same concentration of target cations and different pH values varying from 1 to 14. The results are shown in Figure S1. It can be seen that the $K_4Nb_6O_{17}$ nanolamina can stay ion exchangeable in a light acidic environment. Even when the pH value equals to 1, the adsorbent can still keep half of its equilibrium capacity to adsorb Sr^{2+} or Cs^+ . But for Ba^{2+} cations, the sorption does not happen when the pH value is lower than 2. These results indicate that the $K_4Nb_6O_{17}$ nanolamina is suitable for removing radioactive ions from lightly acidic solutions.

$K_4Nb_6O_{17}$ nanolamina can be manufactured in large scale through a hydrothermal reaction between KOH and niobium sources at low cost, and possess a flexible layered structure which guarantees a relatively high and stable cation exchange capacity for radioactive cations such as Sr^{2+} , Ba^{2+} and Cs^+ . Compared with traditional ion exchanger, $K_4Nb_6O_{17}$ nanolamina is more efficient and prompt as adsorbent to remove these toxic cations from contaminated water. With the presence of competitive K^+ ions in a solution, $K_4Nb_6O_{17}$ can selectively adsorb the toxic cations even when the concentration of K^+ ions is higher than that of the target cations. More importantly, there was a structure deformation of $K_4Nb_6O_{17}$ after ion exchange procedure. This structure deformation results in a permanent trapping of the radioactive ions between the interlayers and thus avoids second contamination during subsequent disposal. Also, the $K_4Nb_6O_{17}$ nanolamina can stay active in a lightly acidic environment

Table 1 | K_d values of Sr^{2+} , Ba^{2+} and Cs^+ sorption by $K_4Nb_6O_{17}$ nanolamina

C_K^* (mol/L)	Sr^{2+} (200 ppm)	Ba^{2+} (500 ppm)	Cs^+ (150 ppm)
0	1060	730	3080
0.01	670	650	960
0.05	640	610	700
0.1	530	520	540

* C_K is the concentration of KCl or KNO_3 in a solution.



and can be separated from water by low-costly filtration, sedimentation or centrifugation. In summary, the $K_4Nb_6O_{17}$ nanolaminas with layered structure are promising candidates as adsorbents for the removal of radioactive cations from water.

Methods

Synthesis. The $K_4Nb_6O_{17}$ nanolaminas were synthesized by the reaction between concentrated KOH solution and niobium pentoxide (Nb_2O_5) under hydrothermal conditions¹⁴. Specifically, 4 g of Nb_2O_5 was dissolved in 80 mL of 0.5 M KOH solution under stirring 1 h. Seal the suspension in a Teflon-lined stainless autoclave at 180°C for 96 h (hydrothermal reaction) to yield potassium niobate nanolaminas. After the hydrothermal procedure the white solid in the autoclaved mixture was recovered and washed with deionized water. Finally, the washed powder was dried at 80°C.

Adsorption test. Considering the high toxicity of $^{90}Sr^{2+}$ and $^{137}Cs^+$, the sorption experiments were carried out using the aqueous solution of their nonradioactive isotopes. Ba^{2+} was also used instead of $^{226}Ra^{2+}$ for the same reason, because these two ions have similar ionic diameters and ion exchange behavior²⁰. The sorption isotherms of metal cations (Sr^{2+} , Ba^{2+} , and Cs^+) sorption were determined at room temperature by equilibrating 100 mg $K_4Nb_6O_{17}$ with 100 mL $Sr(NO_3)_2$, $Ba(NO_3)_2$ or $CsCl$ solution with different concentrations for 48 h. To avoid the effect of the formation of $SrCO_3$ or $BaCO_3$, the pH value of the mixtures were kept in the range of 6 to 7. After the sorption experiments the solid and liquid phase were separated by centrifugation for further characterizations.

Characterization. The surface morphology and composition of the $K_4Nb_6O_{17}$ nanolaminas were obtained on a scanning electron microscope (SEM; Hitachi, S-4800 with an accelerating voltage of 5 kV) and energy-dispersive X-ray spectroscopy (EDX) attached to the used SEM. High-resolution transmission electron microscopy (HRTEM) images were taken on a JEOL JEM-2100F field emission electron microscope under an accelerating voltage of 200 kV. The crystallized phases were identified by powder X-ray diffraction (XRD) analysis using an X-ray diffractometer (DX-2700, China) with Ni-filtered $Cu K\alpha$ radiation ($\lambda = 1.5406 \text{ \AA}$) at 40 kV and 30 mA with a fixed slit. The concentrations of the toxic cations were determined by atomic adsorption spectroscopy (AAS, TAS 990, China).

- Komarneni, S. & Roy, R. A Use of γ -zirconium phosphate for Cs removal from radioactive waste. *Nature* **239**, 707–708 (1982).
- Komarneni, S. & Roy, R. A Cesium-Selective Ion Sieve Made by Topotactic Leaching of Phlogopite Mica. *Science* **239**, 1286–1288 (1988).
- Paulus, W. J., Komarneni, S. & Roy, R. Bulk synthesis and selective exchange of strontium ions in $Na_4Mg_6Al_4Si_4O_{20}F_4$ mica. *Nature* **357**, 571–573 (1992).
- Komarneni, S., Kozai, N. & Paulus, W. J. Superselective Clay for Radium Uptake. *Nature* **410**, 771–772 (2001).
- Nyman, M. *et al.* A New Family of Octahedral Molecular Sieves: Sodium Ti/Zr^{IV} Niobates. *J. Am. Chem. Soc.* **123**, 1529–1530 (2001).
- Nyman, M. *et al.* Sandia Octahedral Molecular Sieves (SOMS): Structural and Property Effects of Charge-Balancing the M^{IV}-Substituted (M = Ti, Zr) Niobate Framework. *J. Am. Chem. Soc.* **124**, 1704–1713 (2002).
- Amphlett, C. B., McDonald, L. A. & Redman, M. J. Synthetic inorganic ion-exchange materials-I zirconium phosphate. *J. Inorg. Nucl. Chem.* **6**, 220–235 (1958).
- Misaelides, P. Application of natural zeolites in environmental remediation: A short review. *Micro. Meso. Mater.* **144**, 15–18 (2011).
- Behrens, E. A., Sylvester, P. & Clearfield, A. Assessment of a Sodium Nonatitanate and Pharmacosiderite-Type Ion Exchangers for Strontium and Cesium Removal from DOE Waste Simulants. *Environ. Sci. Technol.* **32**, 101–107 (1988).
- Bancroft, G. M. *et al.* Surface studies on a leached sphene glass. *Nature* **299**, 708–710 (1982).
- Yang, D., Zheng, Z., Zhu, H., Liu, H. & Gao, X. Titanate Nanofibres as Intelligent Adsorbents for the Removal of Radioactive Ions from Water. *Adv. Mater.* **20**, 2777–2781 (2008).
- Yang, D. *et al.* Layered Titanate Nanofibres as Efficient Adsorbents for Removal of Toxic Radioactive and Heavy Metal Ions from Water. *J. Phys. Chem. C* **122**, 16275–16280 (2008).

- Yang, D. *et al.* Sorption Induced Structural Deformation of Sodium Hexa-titanate Nanofibres and Their Ability to Selectively Trap Radioactive Ra(II) Ions from Water. *Phys. Chem. Chem. Phys.* **12**, 1271–1277 (2010).
- Yang, D. *et al.* Capturing Radioactive Cs⁺ and I⁻ from Water with Titanate Nanofibers and Nanotubes. *Angew. Chem. Int. Ed.* **50**, 10594–10598 (2011).
- Yang, D. *et al.* Titanate-based adsorbents for radioactive ions entrapment from water. *Nanoscale* **5**, 2232–2242 (2013).
- Yang, D. *et al.* Silver oxide nanocrystals anchored on titanate nanotubes and nanofibers: promising candidates for entrapment of radioactive iodine anions. *Nanoscale* **5**, 11011–11018 (2013).
- Liu, J., Li, X. & Li, Y. Synthesis and characterization of nanocrystalline niobates. *J. Cryst. Growth* **247**, 419–424 (2003).
- Ma, J. J. *et al.* Synthesis, characterization and electrochemical behavior of cationic iron porphyrin intercalated into layered niobate. *Micro. Meso. Mater.* **151**, 325–329 (2012).
- Bizeto, M. A., Shiguihara, A. L. & Constantino, V. R. L. Layered niobate nanosheets: building blocks for advanced materials assembly. *J. Mater. Chem.* **19**, 2512–2525 (2009).
- Nassau, K., Shiever, J. W. & Bernstein, J. L. Crystal Growth and Properties of Mica-Like Potassium Niobates. *J. Electrochem. Soc.* **116**, 348–353 (1969).
- Kinomura, N., Kumada, N. & Muto, F. Ion Exchange of $K_4Nb_6O_{17} \cdot H_2O$. *Dalton Trans.* **11**, 2349–2351 (1985).
- Jurado-Vargas, M. *et al.* Ion exchange of radium and barium in zeolites. *J. Radioanaly. Nucl. Chem.* **218**, 153–156 (1997).
- Sawhney, B. Regularity of Interstratification as Affected by Charge Density in Layer Silicates. *Soil Sci. Soc. Am. Proc.* **33**, 42–46 (1969).
- Shainberg, I. & Kemper, W. Hydration Status of Adsorbed Cations. *Soil Sci. Soc. Am. Proc.* **30**, 707–713 (1966).
- Sawhney, B. Selective Sorption and Fixation of Cations by Clay Minerals: A Review. *Clays Clay Miner.* **20**, 93–100 (1972).
- Nightingale, Jr, E. R. Phenomenological Theory of Ion Solvation. Effective Radii of Hydrated Ions. *J. Phys. Chem.* **63**, 1381–1387 (1959).
- Zheng, Z., Philip, C. V., Anthony, R. G. *et al.* Ion Exchange of Group I Metals By Hydrous Crystalline Silicotitanates. *Ind. Eng. Chem. Res.* **35**, 4246–4256 (1996).
- Sarina, S., Bo, A., Liu, D. *et al.* Separate or Simultaneous Removal of Radioactive Cations and Anions from Water by Layered Sodium Vanadate-Based Sorbents. *Chem. Mater.* **26**, 4788–4795 (2014).

Acknowledgments

This work is financially supported by the National Natural Science Foundation of China (No. 21207073) and ARC Discovery Project (Grant no.130104759).

Author contributions

J.S., C.S. and L.L. performed the most experiments. S.Y., R.C. and Y.J. helped conduct the characterization of the adsorbents. D.Y. and X.Y. conceived the project. All authors discussed the results. D.Y. wrote the manuscript.

Additional information

Supplementary information accompanies this paper at <http://www.nature.com/scientificreports>

Competing financial interests: The authors declare no competing financial interests.

How to cite this article: Sun, J. *et al.* Potassium Niobate Nanolamina: A Promising Adsorbent for Entrapment of Radioactive Cations from Water. *Sci. Rep.* **4**, 7313; DOI:10.1038/srep07313 (2014).



This work is licensed under a Creative Commons Attribution-NonCommercial-ShareAlike 4.0 International License. The images or other third party material in this article are included in the article's Creative Commons license, unless indicated otherwise in the credit line; if the material is not included under the Creative Commons license, users will need to obtain permission from the license holder in order to reproduce the material. To view a copy of this license, visit <http://creativecommons.org/licenses/by-nc-sa/4.0/>